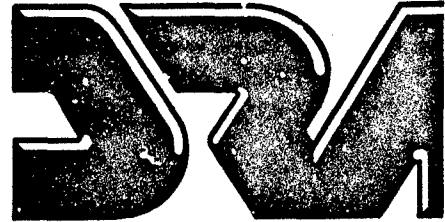


AD-A262 348



OCTOBER 1992

COPY No. 3

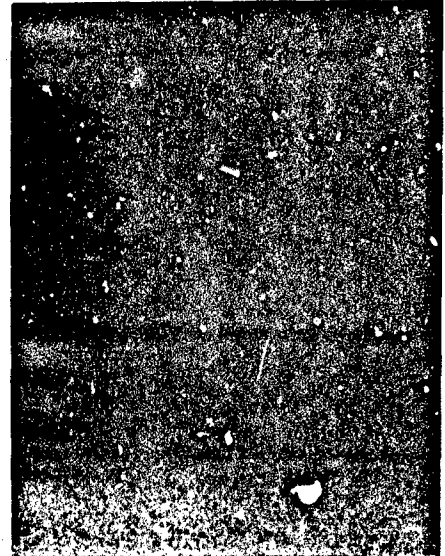


DEFENCE RESEARCH AGENCY

DRA Haslar, Gosport, Hants PO12 2AG

20000920011

SOUND RADIATION
FROM INFINITE LAMINATED
COMPOSITE SHELL WITH
PERIODIC RIB STIFFENING



Reproduced From
Best Available Copy

DTIC
SELECTE
MAR 04 1993
S B D

J H James

DISTRIBUTION STATEMENT A
Approved for public release
Distribution Unlimited

DRA/TMUSGR192326

93-04529



2708

Technical Memorandum

© British Crown Copyright 1992

UNLIMITED

93 3 3 005

0139870

CONDITIONS OF RELEASE

315174

.....

DRIC U

CROWN COPYRIGHT (c)
1992
CONTROLLER
HMSO LONDON

.....

DRIC Y

Reports quoted are not necessarily available to members of the public or to commercial organisations.

DRA TM(USGR)92326

October 1992

**SOUND RADIATION FROM INFINITE LAMINATED COMPOSITE SHELL
WITH PERIODIC RIB STIFFENING**

By J H James

Approved for release

A. V. R. D.

Head of Noise Control Group

SUMMARY

A theory of sound radiation from an infinite cylindrical shell which is stiffened periodically by ribs is given. Both shell and ribs are laminated composites. The shell is modelled by the differential equations of a thin shell theory. The flexible ribs, which exert both forces and moments on the shell's surface, are modelled by thin conical shell finite elements; degrees of freedom other than those at the shell's surface are removed by receptance methods. Excitations are time-harmonic mechanical forces at arbitrary points on the shell's surface and ribs, and acoustic monopoles in the exterior and interior fluids.

DTIC QUALITY INSPECTED 1

Defence Research Agency
Haslar Gosport Hants PO12 2AG

Copyright
Controller HMSO London
1992

Accession For	
NTIS GRA&I	<input checked="" type="checkbox"/>
DTIC TAB	<input type="checkbox"/>
Unannounced	<input type="checkbox"/>
Justification	
By	
Distribution/	
Availability Codes	
Dist	Avail and/or Special
A-1	

INTENTIONALLY LEFT BLANK

CONTENTS LIST	PAGE
TITLE PAGE	i
LIST OF CONTENTS	iii
1. INTRODUCTION	1
2. MATHEMATICS OF PROBLEM	2
2.1. Fourier Transforms	2
2.2. Spectral Response of Shell	2
2.3. Far Field Sound Radiation	3
2.4. Mechanical Excitation on Shell Surface	3
2.5. Mechanical Excitation on Rib	3
2.6. Acoustical Excitation	4
3. NUMERICAL EXAMPLES	5
3.1. General	5
3.2. Isotropic Cylinder	5
3.3. Fibre Reinforced Cylinder	6
3.4. Comparison with an Exact Theory	6
4. CONCLUDING REMARKS	7
REFERENCES	9
FIGURES	11-15
ANNEXES:	
A. Spectral Dynamic Receptance of Shell	A-1 - A-4
B. Dynamic Stiffness Matrix of Rib	B-1 - B-5
DISTRIBUTION	
REPORT DOCUMENTATION PAGE	

SOUND RADIATION FROM INFINITE LAMINATED COMPOSITE SHELL WITH PERIODIC RIB STIFFENING

1. INTRODUCTION

An increasing use of laminated fibre reinforced materials as components in marine vehicles, see, for example, Smith [1], means that well-established theoretical models based on isotropic materials must be re-worked to a certain extent to include anisotropy. The particular problem studied here is the sound radiation from a laminated composite cylindrical shell which is stiffened periodically by identical ribs with flexible cross-sections. The aim is to extend previous theoretical formulations to cover laminated composite materials, flexible ribs of arbitrary cross-section, interior and exterior acoustic excitation, and mechanical excitation on a rib.

Sound radiation from stiffened isotropic thin shells has been studied theoretically by several authors. Conversion of subsonic non-radiating wavenumbers, at the ribs, to supersonic radiating wavenumbers is recognised as an important source of sound radiation with quasi-resonance characteristics. In Bernblit [2] the rib is modelled as a simple circular beam which interacts with the shell through radial forces only; excitations are radial forces on the shell's surface. In James [3] a matrix formulation is given which allows the rib (and excitations) to exert axial, tangential and radial forces together with a meridional moment on the shell's surface; the rib is modelled as a circular beam whose centroid may be offset from the shell's surface; subsequent unpublished work modelled a flexible rib by the finite element method. In Burroughs [4] a doubly periodic arrangement of ribs is considered; the ribs, which are assumed to interact with the shell through radial forces only, are modelled as beams with coupled radial and tangential motion; excitations are radial forces on the shell's surface. In Burroughs and Hallender [5] the previous work has been extended to cover several different types of mechanical excitation on the shell's surface. In Hodges et al. [6] free wave propagation on an unloaded cylinder is examined; in order to give the ribs some measure of flexibility, the web of their "T-rib" is modelled with cubic variation for its axial displacement; this model has been substantially updated by Brazier-Smith and Scott, unpublished work 1988, Topexpress Ltd, to include far field sound radiation and certain hydroacoustic noise sources as excitation. References to other relevant work, particularly on wave propagation in and sound radiation by stiffened plates, are contained in the articles cited.

The geometry is shown in Figure 1. A thin cylindrical shell is stiffened by periodically spaced identical axisymmetric ribs. The cross-section of a rib, shown as a "T-rib" in the diagram, is composed of thin elements. Excitations are time-harmonic mechanical forces on the shell's surface and ribs, and time-harmonic acoustic monopoles in the exterior and interior acoustic fluids. The effect of sound scattering by the finite sized ribs is neglected, ie for the purposes of calculating the acoustic pressure inside the shell the ribs are regarded as line attachments. Both shell and ribs are laminated composites comprising fibre reinforced thin layers with arbitrary stacking angles. In Figure 2(a) is shown the through thickness lamination, as a planar stack of layers; in Figure 2(b) is shown the stacking angle of a typical composite layer, the directions (ϕ, z) on the shell's surface being shown in parentheses.

The work described herein was done under item AS02EH14 of the Strategic Research Programme. It contributes to the first milestone.

2. MATHEMATICS OF PROBLEM

2.1. Fourier Transforms

Field quantities are represented by Fourier integral transforms in the axial direction and Fourier series transforms in the circumferential direction; for example, the function $P(r, \phi, z)$ is expressed as

$$P(r, \phi, z) = (1/2\pi) \sum_{n=-\infty}^{\infty} e^{in\phi} \int_{-\infty}^{\infty} \bar{P}(r, n, \alpha) e^{i\alpha z} d\alpha, \quad (2.1.1)$$

where the spectral quantity is given by the inverse transform

$$\bar{P}(r, n, \alpha) = (1/2\pi) \int_0^{2\pi} e^{-in\phi} \int_{-\infty}^{\infty} P(r, \phi, z) e^{-i\alpha z} dz d\phi. \quad (2.1.2)$$

Fourier transforms facilitate solution of linear differential equations by replacing them with linear algebraic equations. In these and subsequent equations the time variation $e^{-i\omega t}$ is suppressed. Hereafter, bars on spectral quantities will be omitted to simplify notation; the arguments of a function are sufficient to identify it as a Fourier series or Fourier integral transform.

2.2. Spectral Response of Shell

Let $u(\phi, z) = \{u_z(\phi, z), u_\phi(\phi, z), u_r(\phi, z), \psi_\phi(\phi, z)\}^T$ denote a 4×1 column vector of axial, tangential and radial displacements and meridional rotation of the shell's midsurface. From now on, references to a displacement vector implicitly includes the meridional rotation, and references to an excitation vector implicitly includes the meridional moment. The spectral displacements, using general thin shell and rib equations of motion, have been obtained by James [3] as the 4×4 matrix equation

$$u(n, \alpha) = D(n, \alpha)E(n, \alpha) - (1/d)D(n, \alpha)B(n) \times \left\{ \left[I + (1/d) \sum_{q=-\infty}^{\infty} L(n, \alpha + 2\pi q/d)B(n) \right]^{-1} \sum_{q=-\infty}^{\infty} D(n, \alpha + 2\pi q/d)E(n, \alpha + 2\pi q/d) \right\}, \quad (2.2.1)$$

where $u(n, \alpha) = \{u_z(n, \alpha), u_\phi(n, \alpha), u_r(n, \alpha), \psi_\phi(n, \alpha)\}^T$ is the 4×1 column vector of spectral displacements of the shell's midsurface; $D(n, \alpha)$ is a 4×4 spectral receptance matrix whose elements, given in Annex A, depend only on the shell and fluid parameters; $E(n, \alpha)$ is a 4×1 spectral excitation matrix whose elements are obtained from the external excitation matrix $E(\phi, z) = \{E_z(\phi, z), E_\phi(\phi, z), E_r(\phi, z), M_\phi(\phi, z)\}^T$ in which $E_z(\phi, z)$, $E_\phi(\phi, z)$ and $E_r(\phi, z)$ are axial, tangential and radial external stresses and $M_\phi(\phi, z)$ is the meridional moment excitation per unit area; d is the distance between ribs; $B(n)$ is a 4×4 spectral stiffness matrix of a rib whose elements when it is modelled as a beam are given in reference [3] and whose elements when it is modelled by thin axisymmetric conical shell finite elements are derived according to principles described in Annex B; I is a 4×4 identity matrix. Inspection of the above equation shows that the spectral displacement matrix is composed of two terms: the first term, of axial wavenumber α is the spectral displacement of the shell in the absence of ribs; the second term comprises discrete axial wavenumbers $\alpha + 2\pi q/d$ due to various interactions between the periodically spaced ribs, via the shell and its interior and exterior fluids.

2.3. Far Field Sound Radiation

The sound radiation in the exterior fluid, due to a prescribed spectral radial displacement $u_r(n, \alpha)$ of the shell's surface,

$$p(r, \phi, z) = \frac{\rho_e \omega^2}{2\pi} \sum_{n=-\infty}^{\infty} e^{in\phi} \int_{-\infty}^{\infty} [u_r(n, \alpha) H_{|n|}(\gamma_e r) / \gamma_e H'_{|n|}(\gamma_e a)] e^{i\alpha z} d\alpha, \quad (2.3.1)$$

and its stationary phase value in the acoustic far field, $R \rightarrow \infty$,

$$p_f(R, \theta, \phi) = \frac{-i\rho_e \omega^2 \exp(ik_e R)}{\pi k_e R \sin\theta} \sum_{n=-\infty}^{\infty} [(-i)^{|n|} u_r(n, k_e \cos\theta) / H'_{|n|}(k_e a \cos\theta)] e^{in\phi}, \quad (2.3.2)$$

are results that are a standard to acoustics (see, for example, references [7] and [8]). In these equations ρ_e is the density of the exterior fluid; $\gamma_e = +\sqrt{(k_e^2 - \alpha^2)}$; $k_e = \omega/c_e$ is the acoustic wavenumber in the exterior fluid where c_e is sound speed; H_n is the Hankel function $J_n + iY_n$ and the prime on the Hankel function denotes differentiation with respect to its argument; (R, θ, ϕ) are spherical coordinates related to cylindrical coordinates by $z = R \cos(\theta)$, $r = R \sin(\theta)$; $u_r(n, k_e \cos\theta)$ is the third element of the spectral displacement vector of equation (2.2.1) evaluated at wavenumber $\alpha = k_e \cos\theta$. Provided that there is some dissipation, however small, in the shell and ribs, the method of stationary phase is valid formally for all values of θ and ϕ .

2.4. Mechanical Excitation on Shell Surface

The basic external excitation (stress on the shell's surface is the point force and meridional point moment excitation vector, $F = (F_z, F_\phi, F_r, M_\phi)^T$, located at coordinates (a, ϕ_0, z_0) . In this case

$$E(\phi, z) = F \delta(z - z_0) \delta(\phi - \phi_0) / a, \quad (2.4.1)$$

and the spectral excitation is obtained from equation (2.1.2) as

$$E(n, \alpha) = F \exp(-in\phi_0 - i\alpha z_0) / 2\pi a. \quad (2.4.2)$$

2.5. Mechanical Excitation on Rib

A rib is modelled by conical shell finite elements, as shown in Figure 3, the theory being given in Annex B. If there are N nodes on a rib cross-section there are $4N$ degrees of freedom, which could considerably increase the size of the matrices of equation (2.2.1) unless unwanted degrees of freedom are first eliminated. It is assumed that the rib is connected to the shell, along a circumference, at node p , say, where there are four displacements and four excitations which match the shell displacements and excitations. If a mechanical point force F is applied at node q on a flexible rib, then Annex B shows how the method of receptance coupling enables it to be replaced by an equivalent shell excitation at the point p where the rib connects to the shell. This shell excitation is

$$E(n, \alpha) = R_{pp}(n)^{-1} R_{pq}(n) F \exp(-in\phi_p - i\alpha z_p) / 2\pi a, \quad (2.5.1)$$

where $R_{pp}(n)$ and $R_{pq}(n)$ are 4×4 rib receptance matrices. The columns of $R_{pp}(n)$ are the four Fourier series harmonic displacements of the rib at p due to unit harmonic excitation at each in turn of the four excitation degrees of freedom at q . When the points p and q are coincident it is evident that equation (2.5.1) reduces to equation (2.4.2). Thus, provided the excitation is applied at a single node on a flexible rib, the method of receptance coupling allows reduction of the number of rib coupling degrees of freedom from $4N$ to four.

2.6. Acoustical Excitation

A point source located in the interior fluid at coordinates (r_p, ϕ_p, z_p) has free field pressure

$$p_s(r, \phi, z) = p_s \exp(ik_s R_s) / R_s \quad (2.6.1)$$

where $R_s^2 = (z - z_p)^2 + r^2 + r_p^2 - 2rr_p \cos(\phi - \phi_p)$; $k_s = \omega/c_s$ is the wavenumber and c_s is sound speed. Elements of the excitation vector $E(n, \alpha)$ are zero except for [7]

$$E_3 = 2p_s [J_{|n|}(\gamma_s r_p) / \gamma_s a J'_{|n|}(\gamma_s a)] \exp(-in\phi_p - i\alpha z_p), \quad (2.6.2)$$

where $\gamma_s = +\sqrt{(k_s^2 - \alpha^2)}$. The far field sound radiation due to the shell response is given by equation (2.3.2).

When the source is located in the exterior fluid at coordinates (r_p, ϕ_p, z_p) the elements of the excitation vector $E(n, \alpha)$ are again zero except for [7].

$$E_3 = 2p_s [H_{|n|}(\gamma_s r_p) / \gamma_s a H'_{|n|}(\gamma_s a)] \exp(-in\phi_p - i\alpha z_p). \quad (2.6.3)$$

The far field sound radiation due to the shell's response is also given by equation (2.3.2), which must now be augmented by the far field pressure of the source

$$P_{sf}(R, \theta, \phi) = (p_s / R) \exp[ik_s(R - z_p \cos\theta - r_p \sin\theta \cos(\phi - \phi_p))], \quad (2.6.4)$$

and the far field pressure of its rigid boundary reflection [7]

$$P_{rf}(R, \theta, \phi) = -(p_s / R) \exp[ik_s(R - z_p \cos\theta)] \times \sum_{n=-\infty}^{\infty} (-i)^{|n|} [J'_{|n|}(k_s a \sin\theta) H_{|n|}(k_s r_p \sin\theta) / H'_{|n|}(k_s a \sin\theta)] \exp(in(\phi - \phi_p)). \quad (2.6.5)$$

3. NUMERICAL EXAMPLES

3.1. General

A Fortran program has been written to calculate the far field sound radiation from a ribbed laminated shell for both acoustical and mechanical time-harmonic excitation. In order to provide a test of the capability of this program an air, $\rho_1=1.21$, $c_1=343$, filled cylinder, radius $a = 0.10$, thickness $h = 0.002$, excited by a unit rms mechanical point force and radiating into water, $\rho_2=1000$, $c_2=1500$, has been considered. The cylinder material is either isotropic steel, $E = 195$, $G = 75.6$, $\nu=0.29$, $\rho=7700$, or carbon fibre reinforced plastic (CFRP), $E_{\theta\theta}=202$, $E_{zz}=7.4$, $G_{\theta z}=2.74$, $\nu_{\theta z}=0.320$, $\rho=1520$ when reinforced in the circumferential direction and an interchange of ϕ and z is required when reinforced in the axial direction. The "T-rib" dimensions are web thickness 0.002, web length 0.09, flange length 0.08 and flange thickness 0.002; the rib spacing is $d = 0.04$ and the rib material is either steel or circumferentially reinforced CFRP. All material constants are in SI units with Young's and shear moduli in GN/m². Dissipation in the cylinder and ribs is allowed for by setting Young's and shear moduli to complex values, viz $E=E(1-i\eta_e)$ and $G=G(1-i\eta_g)$, etc where the hysteretic loss factor η_e and η_g are all chosen as 0.02 for the numerical examples.

The angular variation of the far field sound radiation exhibits a complicated variation with the angles θ and ϕ due to the dispersive nature of wave propagation in ribbed cylinders. A feature of this dispersion is that frequency locations of peaks in the radiated sound spectra move as the angle of observation changes. In order to smooth out this complicated spatial variation the acoustic power is plotted in Figures 4-5. The far field pressure is always of the form

$$p_f(R, \theta, \phi) = \exp(ik_2 R) / R \sum_{n=-\infty}^{\infty} A(n, \theta) \exp(in\phi), \quad (3.1.1)$$

and it is not difficult to show that the acoustic power is

$$P_f = (2\pi/\rho_2 c_2) \int_0^\pi \left\{ \sum_{n=-\infty}^{\infty} |A(n, \theta)|^2 \right\} \sin\theta d\theta, \quad (3.1.2)$$

where a customary multiplying factor of 1/2 has been omitted as it is convenient to think of the excitation as rms. This equation is integrated numerically by an extended Simpson's rule. The power level, in dB reference 1 picowatt, is defined as $10\log_{10}(P_f)+120.0$. For computations of acoustic power a maximum of 10 circumferential harmonics (n), 12 axial harmonics (q) and 361 theta increments were used. Symmetry in the ranges $\theta=(0,90)$ and $\theta=(90,180)$ degrees was used to reduce computational times.

3.2. Isotropic Cylinder

In Figure 4(a) is shown sound power levels of an unribbed steel cylinder. When the excitation is a radial force the spectrum is generally smooth and it can be demonstrated that it is substantially independent of the shell parameters. When the excitation is an axial force, power levels are initially much greater than those of the radial force, and thereafter the levels are within 4 dB of each other.

A detailed physical interpretation of features in the plots is not given here, but it is worthwhile recording that certain aspects can be explained qualitatively from wavenumber versus frequency plots, as in James [9]. For example, such plots would show that while there are no dominant acoustically fast radial modes, there are acoustically fast axial modes cutting on at 0, 5, 10 and 15 kHz for the $n = 0, 1, 2$ and 3 harmonics, respectively. Thus, most of the power of the radial force comes from a near field cylinder distortion, while most of the power of the axial force comes from supersonic quasi-axial waves which radiate acoustic energy in very sharp beams centred on coincidence angles which vary with harmonic number, n .

In Figures 4(b) and 4(c) are shown sound power levels of the ribbed shell when the excitations are on the shell's surface, at a rib attachment point, and on one of the ribs, at its flange centre (node 4 in Figure 3), respectively. When the excitation is a radial force, there is no noticeable difference between the plots, as the frequency is too low for web longitudinal resonances or flange bending resonances to occur. The broad hump at 10 kHz is more than 10 dB above the corresponding level of the unribbed shell. It is due mainly to a near field effect caused by increased circumferential stiffness of the ribbed shell, together with conversion of subsonic wavenumbers at the ribs into supersonic radiating wavenumbers, the latter effect being more noticeable in sound pressure versus frequency plots for selected θ and ϕ angles. When the excitation is an axial force there is a large increase in power level when the excitation is applied to a rib web rather than to the shell's surface, most certainly due to resonant bending of the web cross-section.

3.3. Fibre Reinforced Cylinder

In Figure 5(a) is shown sound power levels when the shell is composed of axially reinforced CFRP. When the excitation is a radial force it can be demonstrated that the power levels are generally only a few dB above those that would occur in the absence of the shell. When the excitation is an axial force power levels are on average about 10 dB less, except at frequencies below 5 kHz.

In Figures 5(b) and 5(c) are shown sound power levels of the ribbed shell, the shell being composed of axially reinforced CFRP and the ribs of circumferentially reinforced CFRP; excitations are on the shell's surface, at a rib attachment point, and on one of the ribs, at its flange centre (node 4 in Figure 3), respectively. When the excitation is a radial force, there is no noticeable difference between the plots, except in the range 15-20 kHz where levels are higher when the excitation is on the rib; due presumably to the onset of a web longitudinal resonance. The broad hump at 10 kHz is less dominant than in Figure 4. When the excitation is an axial force there is a large increase in power when the excitation is applied to a rib web rather than to the shell's surface, most certainly due to resonant bending of the web cross-section.

Comparing power levels in Figures 4 and 5 shows that when the excitation is a radial force, levels of the CFRP shell are generally just above those of the steel shell; for axial force excitation, levels of the CFRP are generally considerably less.

3.4. Comparison with an Exact Theory

It is generally agreed that higher order shear deformation theories are necessary for accurate static and dynamic response calculations of laminated composites, which are usually very compliant in transverse shear. Classical plate and shell theory (as used herein) are thought to be inadequate for all but the thinnest of composites; thus, the numerical results shown need to be validated by comparing them with those of a higher order theory. Fortunately, a Fortran program [7] is available for predicting acoustic radiation from cylindrically laminated composites for the case in which the layers are modelled by exact equations of linear anisotropic elasticity.

For the isotropic steel cylinder, exact theory gives numerical values of power which are almost indistinguishable from those shown in Figure 4(a). For the axially reinforced CFRP cylinder, differences between power levels of exact theory and those shown in Figure 5(a) are hardly noticeable. The plots of power obtained from exact theory are not reproduced here. As the thickness of the cylinder is increased, without other constants changing, the differences between exact power levels and those of shell theory will become increasingly apparent, but an assessment of the range of applicability of classical shell theory applied to laminated composites is outside the scope of this theoretical paper. However, provided the composite is sufficiently thin, it is surmised that classical shell theory, used with caution, is adequate for phenomenological numerical studies.

The receptance matrix $S(n, \alpha)$ of the shell and the stiffness matrix $B(n)$ of the rib can also be obtained from the exact theory described in references [7] and [13], respectively. The analysis procedure would not be difficult, but computer times would be an order of magnitude greater.

4. CONCLUDING REMARKS

Previous work on sound radiation from an infinite shell with periodic stiffening has been extended to include fibre reinforced materials, flexible ribs of arbitrary thin-walled cross-section, mechanical excitation on a rib and acoustic excitation by interior and exterior monopoles. The flexible rib which is modelled by conical shell finite elements, usually has a large number of degrees of freedom; the method of receptance coupling has shown how unwanted degrees of freedom can be eliminated. Numerical results have demonstrated that the presence of flexible ribs or anisotropy can substantially change the acoustic power spectrum characteristics. Lengthy parametric studies which include different fibre and matrix materials, stacking angles and stacking sequences will be required to establish physical principles of practical importance. The computer programs developed as part of this study are useful tools for such parametric studies.

For numerical investigations in which the shell contains a finite number of ribs of arbitrary spacing and differing cross-sections, the method of dynamic stiffness coupling as used by James [10] to solve a scattering problem is relevant. For analytical investigations of the physics of sound radiation and scattering the methods of Skelton [11] are appropriate for simple constraints. For finite axisymmetric shells, with internal axisymmetric structure, models based on analytical methods such as in Laulagnet and Guyader [12] or coupled finite element and Helmholtz integral equation formulations as in James [13] enable computations of low frequency sound radiation.

INTENTIONALLY LEFT BLANK

REFERENCES

1. C S Smith 1990. Design of Marine Structures in Composite Materials. London. Elsevier.
2. M V Bernblit 1975. Soviet Physics Acoustics 20(5), 414-418. Sound radiation by a thin elastic cylindrical shell with reinforcing ribs.
3. J H James 1978. Admiralty Marine Technology Establishment, Teddington, AMTE(N)R78404. Sound radiation from an infinite shell with periodic stiffeners.
4. C B Burroughs 1984. Journal of the Acoustical Society of America 75(3), 715-722. Acoustic radiation from fluid-loaded infinite circular cylinders with doubly periodic ring supports.
5. C B Burroughs and J E Hallender 1992. Journal of the Acoustical Society of America 91(5), 2721-2739. Acoustic radiation from fluid loaded, ribbed cylindrical shells excited by different types of concentrated mechanical drives.
6. C H Hodges, J Power and J Woodhouse 1985. Journal of Sound and Vibration 101(2), 219-235. The low frequency vibration of a ribbed cylinder, Part 1: theory.
7. E A Skelton and J H James 1992. Journal of Sound and Vibration. Accepted for Publication. Acoustics of an anisotropic layered cylinder.
8. M C Junger and D Feit 1986. Sound, Structures and Their Interaction (second edition). Cambridge, Massachusetts: the MIT Press.
9. J H James 1981. Admiralty Marine Technology Establishment, Teddington, TM81048. Sound radiation from fluid-filled pipes.
10. J H James 1985. Admiralty Research Establishment, Teddington, TM85092. Sound scattering by axisymmetric constraints on uniform shell.
11. E A Skelton 1991. Journal of Sound and Vibration 148(2), 243-264. Acoustic scattering by a disk constraining an infinite fluid-loaded cylindrical shell.
12. B Laulagnet and J L Guyader 1990. Journal of Sound and Vibration 138(2), 173-191, Sound radiation by finite cylindrical ring stiffened shells
13. J H James 1992. Defence Research Agency, Report. Manuscript in Preparation. Finite element and Helmholtz integral equation formulation of low frequency acoustics of thin and thick axisymmetric laminated composite shells.
14. A W Leissa and M S Qatu 1991. Journal of Applied Mechanics 58, 181-188. Equations of elastic deformation of laminated composite shallow shells.
15. C C Chamis 1984. SAMPE Quarterly 15, 14-23. Simplified composite micromechanics equations for hygral, thermal and mechanical properties.

16. R M Jones 1975. *Mechanics of Composite Materials*. New York: Hemisphere.
17. J H Percy et al. 1965. *AIAA Journal* 3(11), 2138-2145. Application of matrix displacement method to linear elastic analysis of shells of revolution.

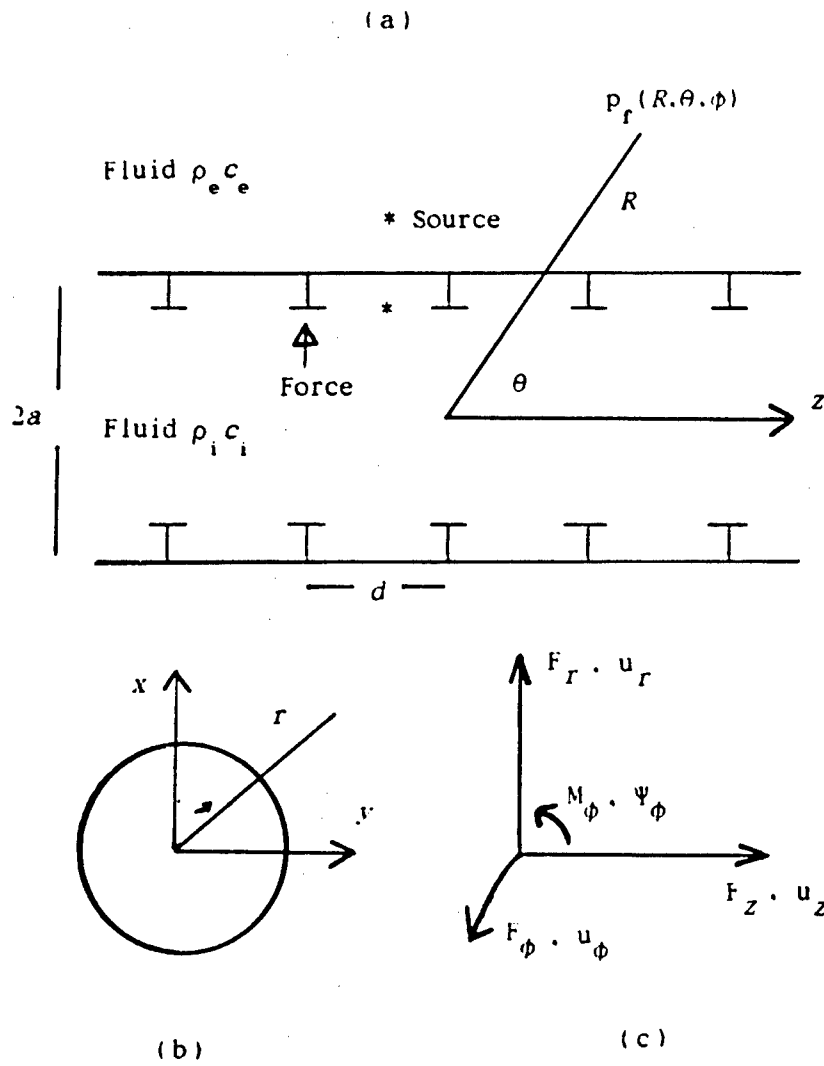


FIGURE 1. (a) PERIODICALLY RIBBED SHELL; (b) COORDINATE SYSTEMS;
 (c) POSITIVE DIRECTIONS OF EXCITATIONS AND DISPLACEMENTS

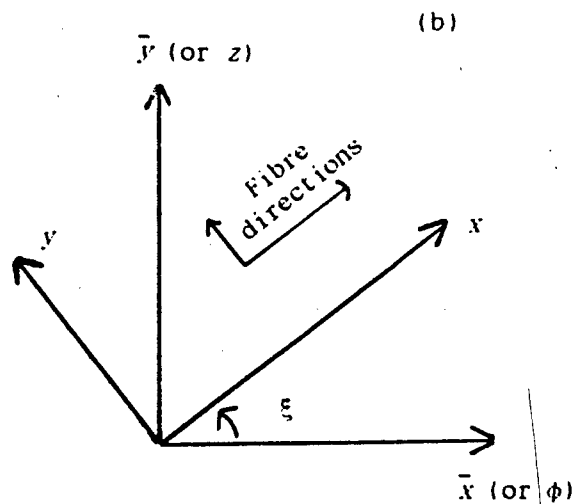
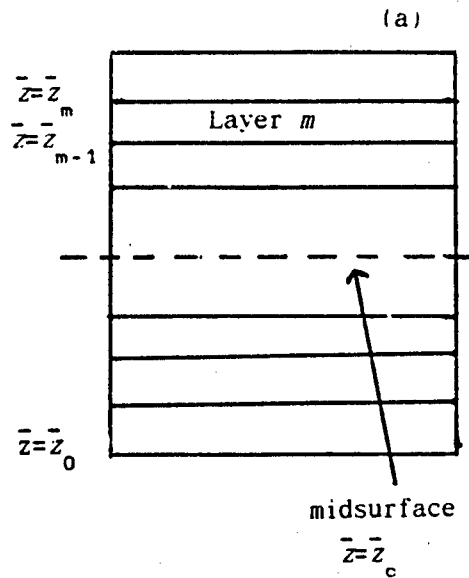


FIGURE 2. (a) LAMINATED COMPOSITE COMPRISING A STACK OF THIN FIBRE REINFORCED PLATES; (b) STACKING ANGLE RELATIVE TO LOCAL (x,y) AND GLOBAL (\bar{x},\bar{y}) COORDINATES, WHICH ARE UNRELATED TO THOSE IN FIGURE 1. ACTUAL CYLINDER (ϕ,z) COORDINATES ARE IN PARENTHESES

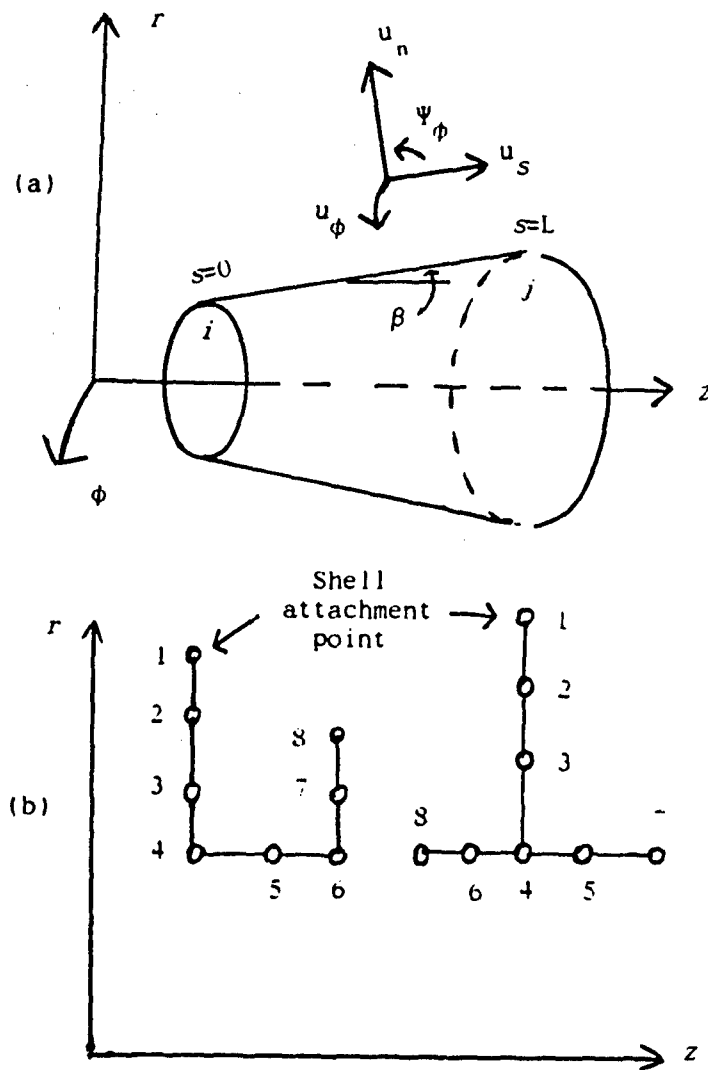


FIGURE 3. (a) CONICAL SHELL FINITE ELEMENT (WITH NODES AT i AND j) AND ITS DISPLACEMENTS IN LOCAL COORDINATES; (b) EXAMPLES OF RIB CROSS-SECTION ASSEMBLED FROM CONICAL SHELL ELEMENTS

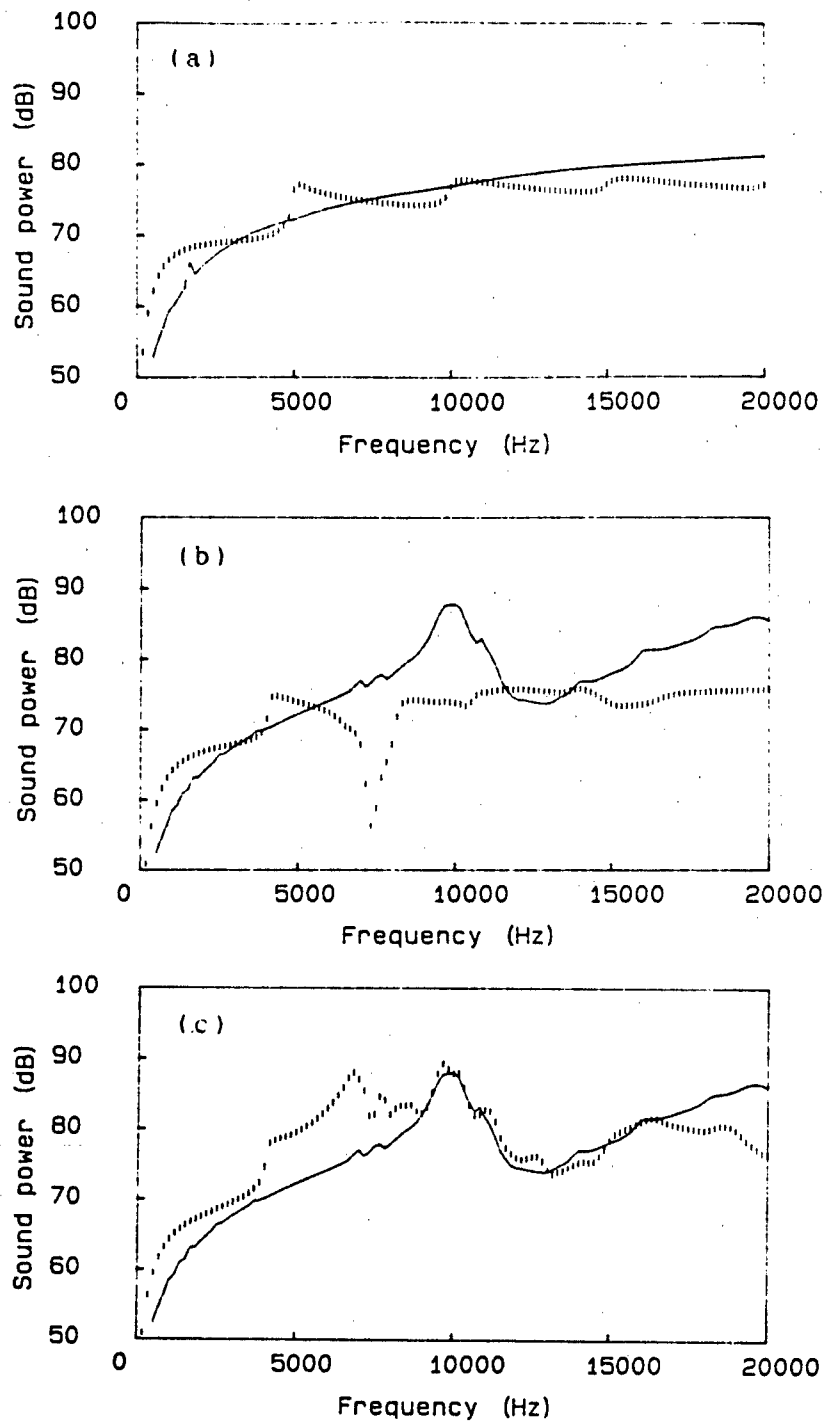
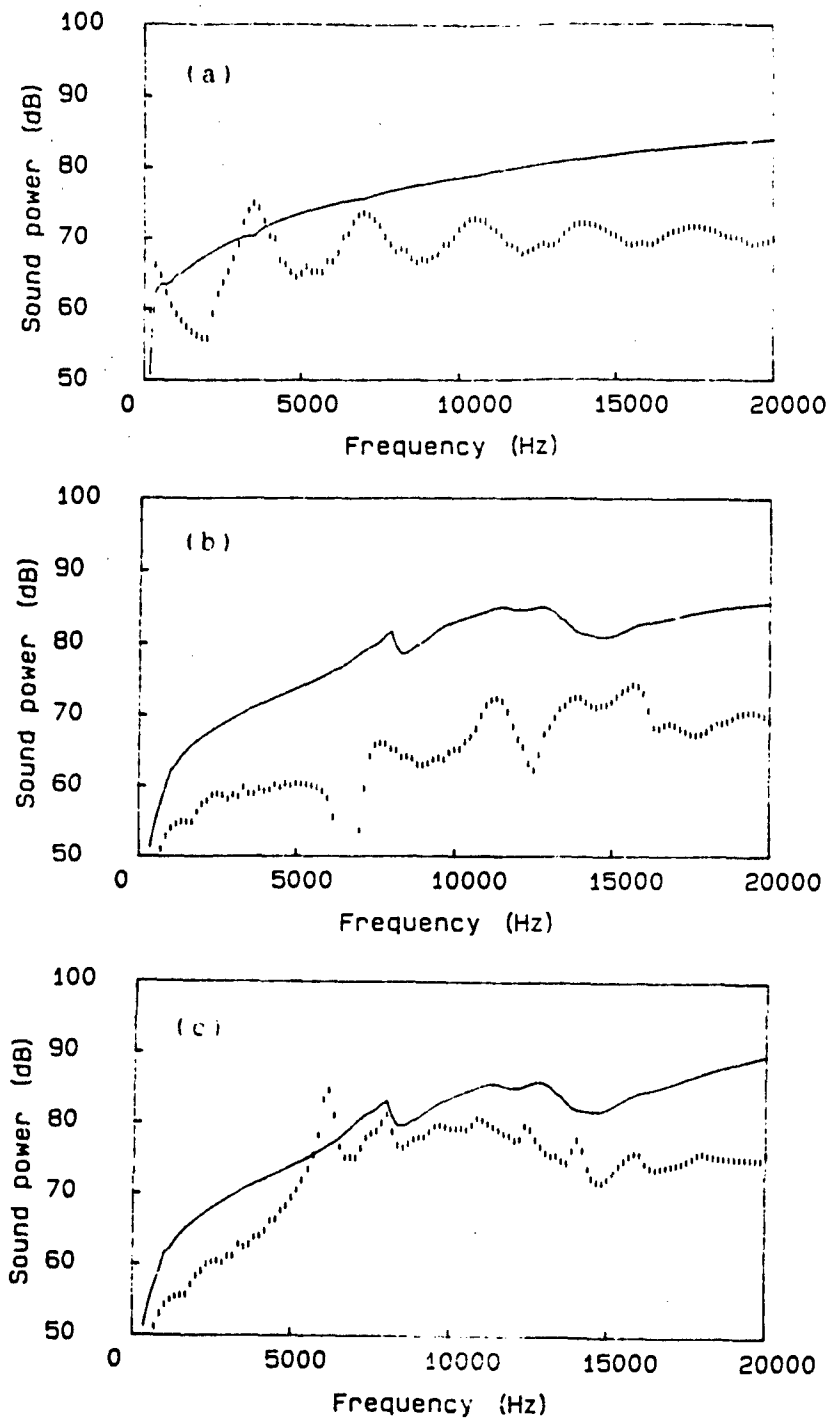


FIGURE 4. ACOUSTIC POWER IN WATER DUE TO ——— RADIAL AND AXIAL POINT FORCE EXCITATION OF AIR FILLED STEEL CYLINDER WITH STEEL T-RIBS; (a) NO RIBS; (b) RIBS, FORCE ON SHELL AT RIB CONNECTION POINT; (c) RIBS, FORCE ON RIB AT FLANGE CENTRE



**FIGURE 5. ACOUSTIC POWER IN WATER DUE TO ——— RADIAL AND AXIAL POINT FORCE EXCITATION OF AIR FILLED AXIALLY REINFORCED CFRP CYLINDER WITH CIRCUMFERENTIALLY REINFORCED CFRP T-RIBS;
 (a) NO RIBS; (b) RIBS, FORCE AT RIB CONNECTION POINT;
 (c) RIBS, FORCE ON RIB AT FLANGE CENTRE**

INTENTIONALLY LEFT BLANK

Annex A

SPECTRAL DYNAMIC RECEPTANCE OF SHELL

A1. Differential Equations

The shell equations of motion are expressed in operator form as

$$\begin{pmatrix} L_{11} & L_{12} & L_{13} \\ L_{21} & L_{22} & L_{23} \\ L_{31} & L_{32} & L_{33} \end{pmatrix} \begin{pmatrix} u_z(\phi, z) \\ u_\phi(\phi, z) \\ u_r(\phi, z) \end{pmatrix} = \begin{pmatrix} E_z(\phi, z) \\ E_\phi(\phi, z) \\ E_r(\phi, z) \end{pmatrix} - \begin{pmatrix} 0 \\ 0 \\ p_e(a, \phi, z) - p_i(a, \phi, z) \end{pmatrix} \quad (\text{A.1.1})$$

where E_z , E_ϕ and E_r are the excitation stresses applied to the midsurface of the shell; they are positive when acting in the positive direction of the coordinate axes. The quantities p_e and p_i are the pressures due to external and internal fluids, respectively. The operators L_{ij} depend on the particular shell theory used. Here the laminated composite shallow shell equations of Leissa and Qatu [14], in which effects due to transverse shear and rotary inertia are neglected, are adopted. The operators, in cylindrical coordinates rather than in the general coordinates used by these authors, are

$$\begin{aligned} L_{11} &= -[A_{66}\partial^2/a^2\partial\phi^2 + 2A_{26}\partial^2/a\partial z\partial\phi + A_{22}\partial^2/\partial z^2] + \rho_s h\partial^2/\partial t^2, \\ L_{12} &= -[A_{16}\partial^2/a^2\partial\phi^2 + (A_{12}+A_{66})\partial^2/a\partial\phi\partial z + A_{26}\partial^2/\partial z^2], \\ L_{13} &= +[B_{16}\partial^3/a^3\partial\phi^3 + 3B_{26}\partial^3/a\partial z^2\partial\phi + (B_{12}+2B_{66})\partial^3/a^2\partial\phi^2\partial z + B_{22}\partial^3/\partial z^3] \\ &\quad - [A_{12}\partial/a\partial z + A_{16}\partial/a^2\partial\phi], \\ L_{22} &= -[A_{11}\partial^2/a^2\partial\phi^2 + 2A_{16}\partial^2/a\partial\phi\partial z + A_{66}\partial^2/\partial z^2] + \rho_s h\partial^2/\partial t^2, \\ L_{23} &= +[B_{11}\partial^3/a^3\partial\phi^3 + 3B_{16}\partial^3/a^2\partial\phi^2\partial z + (B_{12}+2B_{66})\partial^3/a\partial\phi\partial z^2 + B_{26}\partial^3/\partial z^3] \\ &\quad - [A_{11}\partial/a^2\partial\phi + A_{16}\partial/a\partial z], \\ L_{33} &= +[D_{11}\partial^4/a^4\partial\phi^4 + 4D_{16}\partial^4/a^3\partial z\partial\phi^3 + 2(D_{12}+2D_{66})\partial^4/a^2\partial z^2\partial\phi^2 + 4D_{26}\partial^4/a\partial\phi\partial z^3 + D_{22}\partial^4/\partial z^4] \\ &\quad + A_{11}/a^2 - [2B_{11}\partial^2/a^3\partial\phi^2 + 4B_{16}\partial^2/a^2\partial z\partial\phi + 2B_{12}\partial^2/a\partial z^2] + \rho_s h\partial^2/\partial t^2, \\ L_{21} &= L_{12} \quad L_{31} = -L_{13} \quad L_{32} = -L_{23} \end{aligned} \quad (\text{A.1.2})$$

where ρ_s is the mean density of the shell and h is its thickness. When the shell consists of a single isotropic layer it can be shown that these operators reduce to those of the baseline cylindrical shell theory of Donnell and Mushtari [8].

A2. Stiffness Values

The stiffness values A_y , B_y and D_y are the same as those derived from laminated composite plate theory. The laminated plate comprises M thin layers, see Figure 2, of fibre reinforced orthotropic material. For the equivalent lamination on the shell's surface identify the global \bar{x} and \bar{y} axis with the cylindrical ϕ and z axes, respectively. In the local x - y plane a typical layer has "engineering" elastic constants: E_{xx} and E_{yy} the Young's moduli; G_{xy} the shear modulus; ν_{xy} and ν_{yx} the Poisson's ratios which are related by the symmetry relation $E_{xx}/\nu_{xy} = E_{yy}/\nu_{yx}$. For unidirection fibre reinforcement in an isotropic matrix material simple mixture theories such as the one proposed by Chamis [15] enable these constants to be found from the elastic constants of the component materials. In the global \bar{x} - \bar{y} axes set the orthotropic constants of a layer are obtained from the plane stress matrix relation

$$\begin{vmatrix} \bar{\sigma}_x \\ \bar{\sigma}_y \\ \bar{\tau} \end{vmatrix} = \begin{vmatrix} \bar{Q}_{11} & \bar{Q}_{12} & \bar{Q}_{16} \\ \bar{Q}_{12} & \bar{Q}_{22} & \bar{Q}_{26} \\ \bar{Q}_{16} & \bar{Q}_{26} & \bar{Q}_{66} \end{vmatrix} \begin{vmatrix} \bar{\epsilon}_x \\ \bar{\epsilon}_y \\ \bar{\gamma}_{xy} \end{vmatrix} \quad (\text{A.2.1})$$

If the layer is stacked at an angle ξ , the elements of this constitutive matrix are obtained from standard transformations, see, for example, Jones [16],

$$\begin{aligned} \bar{Q}_{11} &= Q_{11}\cos^4\xi + 2(Q_{12}+2Q_{66})\sin^2\xi\cos^2\xi + Q_{22}\sin^4\xi, \\ \bar{Q}_{12} &= (Q_{11}+Q_{22}-4Q_{66})\sin^2\xi\cos^2\xi + Q_{12}(\sin^4\xi+\cos^4\xi), \\ \bar{Q}_{16} &= (Q_{11}-Q_{12}-2Q_{66})\sin\xi\cos^3\xi + (Q_{12}-Q_{22}+2Q_{66})\sin^3\xi\cos\xi, \\ \bar{Q}_{22} &= Q_{11}\sin^4\xi + 2(Q_{12}+2Q_{66})\sin^2\xi\cos^2\xi + Q_{22}\cos^4\xi, \\ \bar{Q}_{26} &= (Q_{11}-Q_{12}-2Q_{66})\sin^3\xi\cos\xi + (Q_{12}-Q_{22}+2Q_{66})\sin\xi\cos^3\xi, \\ \bar{Q}_{66} &= (Q_{11}+Q_{22}-2Q_{12}-2Q_{66})\sin^2\xi\cos^2\xi + Q_{66}(\sin^4\xi+\cos^4\xi), \end{aligned} \quad (\text{A.2.2})$$

where

$$Q_{11} = E_x / (1 - \nu_{xy}\nu_{yx}), \quad Q_{22} = E_y / (1 - \nu_{xy}\nu_{yx}), \quad Q_{12} = E_x\nu_{yx} / (1 - \nu_{xy}\nu_{yx}), \quad Q_{66} = G_{xy},$$

are the only non-zero elements of the constitutive matrix in local coordinates.

The stiffness and density constants required in equation (A.1.2) are obtained by summing the layer constants as follows

$$A_y = \sum_{m=1}^M \overline{Q}_y^{(m)}(t_m - t_{m-1}), \quad B_y = \frac{1}{2} \sum_{m=1}^M \overline{Q}_y^{(m)}(t_m^2 - t_{m-1}^2), \quad (A.2.3)$$

$$D_y = \frac{1}{3} \sum_{m=1}^M \overline{Q}_y^{(m)}(t_m^3 - t_{m-1}^3), \quad \rho_s = (1/h) \sum_{m=1}^M \rho^{(m)}(t_m - t_{m-1}),$$

where $t_m = z_m - z_c$ with z_m and z_{m-1} being the z coordinates of the upper and lower surfaces of the (m)th layer; z_c is the z coordinate of the laminate's midsurface; ρ is the layer density; h is the total thickness of the laminate. The stiffness A_y values are related to in-plane stretching of the shell's midsurface; the D_y values to bending of the surface; the B_y values to coupling between bending and stretching. When the shell is laminated symmetrically with respect to its midsurface, the B_y values are zero.

A3. Spectral Dynamic Stiffness

Replace the field quantities in equation (A.1.1) by their Fourier transforms, defined by equation (2.1.1), to give the spectral dynamic stiffness matrix relation

$$\begin{vmatrix} S_{11}(n, \alpha) & S_{12}(n, \alpha) & S_{13}(n, \alpha) \\ S_{21}(n, \alpha) & S_{22}(n, \alpha) & S_{23}(n, \alpha) \\ S_{31}(n, \alpha) & S_{32}(n, \alpha) & S_{33}(n, \alpha) \end{vmatrix} \begin{vmatrix} u_z(n, \alpha) \\ u_\phi(n, \alpha) \\ u_r(n, \alpha) \end{vmatrix} = \begin{vmatrix} E_z(n, \alpha) \\ E_\phi(n, \alpha) \\ E_r(n, \alpha) \end{vmatrix} \quad (A.3.1)$$

where

$$S_{11} = + [A_{66}n^2/a^2 + 2A_{26}n/a + A_{22}\alpha^2] - \rho_s h \omega^2,$$

$$S_{12} = + [A_{16}n^2/a^2 + (A_{12} + A_{66})n/a + A_{26}\alpha^2],$$

$$S_{13} = -i [B_{16}n^3/a^3 + 3B_{26}n^2/a + (B_{12} + 2B_{66})n/a + B_{22}\alpha^3 + A_{12}n/a + A_{16}n/a^2], \quad (A.3.2)$$

$$S_{22} = + [A_{11}n^2/a^2 + 2A_{16}n/a + A_{66}\alpha^2] - \rho_s h \omega^2,$$

$$S_{23} = -i [B_{11}n^3/a^3 + 3B_{16}n^2/a + (B_{12} + 2B_{66})n/a + B_{26}\alpha^3 + A_{11}n/a^2 + A_{16}n/a],$$

$$\begin{aligned}
S_{33} = & + [D_{11}n^4/a^4 + 4D_{16}n^3\alpha/a^3 + 2(D_{12} + 2D_{66})n^2\alpha^2/a^2 + 4D_{26}n\alpha^3/a \\
& + D_{22}\alpha^4 + 2B_{11}n^2/a^3 + 4B_{16}n\alpha/a^2 + 2B_{12}\alpha^2/a + A_{11}/a^2] - \rho_f h \omega^2 \\
& + \rho_e \omega^2 H_n(\gamma_e a) / \gamma_e H'_n(\gamma_e a) - \rho_i \omega^2 J_n(\gamma_i a) / \gamma_i J'_n(\gamma_i a), \\
S_{21} = & S_{12}, \quad S_{31} = -S_{13}, \quad S_{32} = -S_{23}.
\end{aligned}$$

The last two terms of S_{33} are the fluid loading spectral coefficients of the exterior and interior fluids, respectively, see, for example, reference [7].

The solution of equation (A.3.1) is the spectral receptance matrix relating spectral forces and displacements, viz.

$$\begin{vmatrix} u_z(n, \alpha) \\ u_\phi(n, \alpha) \\ u_r(n, \alpha) \end{vmatrix} = \begin{vmatrix} D_{11}(n, \alpha) & D_{12}(n, \alpha) & D_{13}(n, \alpha) \\ D_{21}(n, \alpha) & D_{22}(n, \alpha) & D_{23}(n, \alpha) \\ D_{31}(n, \alpha) & D_{32}(n, \alpha) & D_{33}(n, \alpha) \end{vmatrix} \begin{vmatrix} E_z(n, \alpha) \\ E_\phi(n, \alpha) \\ E_r(n, \alpha) \end{vmatrix} \quad (\text{A.3.3})$$

As a rib is assumed to exert a meridional moment on the shell, in addition to the three orthogonal stresses, it is necessary to expand equation (A.3.3) to include moment excitation per unit area, $M_\phi(\phi, z)$, via its spectral quantity, $M_\phi(n, \alpha)$. The moment excitation is equivalent to a radial stress excitation $-\partial M_\phi(\phi, z) / \partial z$, whose spectral form is $-i\alpha M_\phi(n, \alpha)$; the corresponding meridional rotation, $\Psi_\phi(\phi, z) = \partial u_r(\phi, z) / \partial z$, has spectral form $\Psi_\phi(n, \alpha) = i\alpha u_r(n, \alpha)$. Thus, noting that the elements D_{ij} are interpreted as the spectral response in direction i due to unit spectral excitation in direction j , it can be shown that the expanded matrix relation is

$$\begin{vmatrix} u_z(n, \alpha) \\ u_\phi(n, \alpha) \\ u_r(n, \alpha) \\ \Psi_\phi(n, \alpha) \end{vmatrix} = \begin{vmatrix} D_{11}(n, \alpha) & D_{12}(n, \alpha) & D_{13}(n, \alpha) & D_{14}(n, \alpha) \\ D_{21}(n, \alpha) & D_{22}(n, \alpha) & D_{23}(n, \alpha) & D_{24}(n, \alpha) \\ D_{31}(n, \alpha) & D_{32}(n, \alpha) & D_{33}(n, \alpha) & D_{34}(n, \alpha) \\ D_{41}(n, \alpha) & D_{42}(n, \alpha) & D_{43}(n, \alpha) & D_{44}(n, \alpha) \end{vmatrix} \begin{vmatrix} E_z(n, \alpha) \\ E_\phi(n, \alpha) \\ E_r(n, \alpha) \\ M_\phi(n, \alpha) \end{vmatrix} \quad (\text{A.3.4})$$

where

$$\begin{aligned} D_{14}(n,\alpha) &= -i\alpha D_{13}(n,\alpha), & D_{24}(n,\alpha) &= -i\alpha D_{23}(n,\alpha), \\ D_{34}(n,\alpha) &= -i\alpha D_{33}(n,\alpha), & D_{41}(n,\alpha) &= i\alpha D_{31}(n,\alpha), \\ D_{42}(n,\alpha) &= i\alpha D_{32}(n,\alpha), & D_{43}(n,\alpha) &= i\alpha D_{33}(n,\alpha), \\ D_{44}(n,\alpha) &= \alpha^2 D_{33}(n,\alpha). \end{aligned} \tag{A.3.5}$$

Denote the 4 x 4 coefficient matrix by $D(n,\alpha)$: this is the shell's spectral dynamic receptance matrix which is required in equation (2.2.1).

INTENTIONALLY LEFT BLANK

Annex B

DYNAMIC STIFFNESS MATRIX OF RIB

B1. Finite Element Modelling of Rib

A rib is modelled as an assemblage of axisymmetric conical shell elements, whose versatility is illustrated in Figure 3 which shows examples of rib cross-section which can be generated from these elements.

The theory of a conical shell element is based on the strain definitions in the local surface coordinate system (ϕ, s)

$$\begin{aligned}
 \epsilon_{\phi} &= \partial u_{\phi} / r \partial \phi + (u_n \cos \beta + u_s \sin \beta) / r, \\
 \epsilon_s &= \partial u_s / \partial s, \\
 \gamma_{s\phi} &= \partial u_s / r \partial \phi + \partial u_{\phi} / \partial s - u_{\phi} \sin \beta / r, \\
 \chi_{\phi} &= -\partial^2 u_n / r^2 \partial \phi^2 + \cos \beta \partial u_{\phi} / r^2 \partial \phi - \sin \beta \partial u_n / r \partial s, \\
 \chi_s &= -\partial^2 u_n / \partial s^2, \\
 \tau &= -2\partial^2 u_n / r \partial s \partial \phi + 2\sin \beta (\partial u_n / r^2 \partial \phi + 2\cos \beta (\partial u_{\phi} / r \partial s) - 2\sin \beta \cos \beta (u_{\phi} / r^2)),
 \end{aligned} \tag{B.1.1}$$

where ϵ_{ϕ} and ϵ_s are midsurface normal strains; $\gamma_{s\phi}$ is the shear strain; χ_{ϕ} and χ_s are changes in curvature; τ is twist; u_n , u_{ϕ} and u_s are displacements normal to the surface, around the circumference and along the generator, respectively; β is the slope of the conical shell generator.

The 6 x 6 constitutive matrix D_s , relating stress and moment resultants to midsurface strain, is defined by the matrix relation

$$\begin{array}{c}
 \left| \begin{array}{l} N_{\phi} \\ N_s \\ N_{s\phi} \\ M_{\phi} \\ M_s \\ M_{s\phi} \end{array} \right| = \left| \begin{array}{cccccc} A_{11} & A_{12} & A_{16} & B_{11} & B_{12} & B_{16} \\ A_{12} & A_{22} & A_{26} & B_{12} & B_{22} & B_{26} \\ A_{16} & A_{26} & A_{66} & B_{16} & B_{26} & B_{66} \\ B_{11} & B_{12} & B_{16} & D_{11} & D_{12} & D_{16} \\ B_{12} & B_{22} & B_{26} & D_{12} & D_{22} & D_{26} \\ B_{16} & B_{26} & B_{66} & D_{16} & D_{26} & D_{66} \end{array} \right| \left| \begin{array}{l} \epsilon_{\phi} \\ \epsilon_s \\ \gamma_{s\phi} \\ \chi_{\phi} \\ \chi_s \\ \tau \end{array} \right|
 \end{array} \tag{B.1.2}$$

where the stiffness coefficients have been defined in Annex A.

B2. Mass and Stiffness Matrices of Element

Field quantities are expanded as Fourier series in the circumferential coordinate. Thus, for the function $P(\phi, s)$

$$P(\phi, s) = \sum_{n=-\infty}^{\infty} P(n, s)e^{in\phi} \text{ where } P(n, s) = (1/2\pi) \int_0^{2\pi} P(\phi, s)e^{-in\phi} d\phi. \quad (\text{B.2.1})$$

Because of the orthogonality property of the harmonic functions a finite element analysis can be carried out for each harmonic $P(n, s)$ separately. Thus, the following procedure refers to values in the n th harmonic, and the requirement to sum the Fourier series, over values of n , to obtain the actual field quantity is implicitly assumed. The theory is given with minimal explanation: details for $\cos(n\phi)$ variation are contained in the pioneering paper of Percy et al. [17] and numerous texts on the finite element method; extension of $\exp(in\phi)$ variation as herein is not difficult.

The conical shell displacement $u_\phi(n, s)$ normal to its generator is represented by a cubic in the variable s which is the distance along the generator from node i . The displacement along the generator $u_s(n, s)$ and the displacement around the circumference $u_\theta(n, s)$ are both assumed to vary linearly in the coordinate s . The rotation of the meridian is $\Psi_\phi(n, s) = \partial u_\phi(n, s) / \partial s$. The equation of motion of the element is found by standard finite element procedure as

$$[S_\phi(n) - \omega^2 M_\phi] u_\phi(n) = E_\phi(n), \quad (\text{B.2.2})$$

where

$$S_\phi(n) = 2\pi (A_\phi^{-1})^{*t} \left[\int_{s=0}^L B_\phi^{*t}(n, s) D_\phi B_\phi(n, s) r ds \right] A_\phi^{-1}, \quad (\text{B.2.3})$$

$$M_\phi = 2\pi (A_\phi^{-1})^{*t} \left[\int_{s=0}^L \rho_\phi h_\phi V_\phi(s) r ds \right] A_\phi^{-1}.$$

The 8×8 matrix $S_\phi(n)$ is the stiffness matrix of the element in the n th harmonic; the 8×8 matrix M_ϕ is the mass matrix which is independent of the harmonic number; the superscripts -1 , $*$ and t denote the operations of inverse, complex conjugate and transpose, respectively; the subscript e indicates that the quantity to which it is attached refers to a single conical shell element; the matrices A_ϕ , B_ϕ , and V_ϕ are given below; the 6×6 matrix D_ϕ is the constitutive matrix of equation (B.1.2); ρ_ϕ is the element's density and h_ϕ is its thickness. The integrals are evaluated numerically, by a simple quadrature scheme, to avoid lengthy algebra.

The matrices $u_\phi(n)$ and $E_\phi(n)$ are 8×1 column vectors of nodal displacements and nodal excitations in the global coordinate system, viz

$$u_\phi(n) = \{u_z^t(n), u_\theta^t(n), u_r^t(n), \Psi_\phi^t(n), u_z^t(n), u_\theta^t(n), u_r^t(n), \Psi_\phi^t(n)\}^t,$$

and

$$E_\phi(n) = \{E_z^t(n), E_\theta^t(n), E_r^t(n), M_\phi^t(n), E_z^t(n), E_\theta^t(n), E_r^t(n), M_\phi^t(n)\}^t, \quad (\text{B.2.4})$$

where the superscripts i and j refer to the left and right nodes on the element. For a force vector, $F_i(\phi)$, per unit length in the circumferential direction at node i , the excitation matrix at this node can be shown to be $E^i(n) = 2\pi r_i F_i(n)$, where $F_i(n)$ is obtained from the Fourier transform equation (B.2.1) and r_i is the radial coordinate of the node; the excitation matrix $E^j(n)$ at node j is identically zero if there is no excitation there. Thus, for a point force $F_i(\phi) = F\delta(\phi - \phi_0)/r_i$ applied at node i at $\phi = \phi_0$, the 4×1 excitation matrix is simply $E^i(n) = F \exp(-in\phi_0)$ where the matrix F is defined in Section 2.4.

The non-zero elements of the 6×8 matrix $B_e(n)$ are

$$\begin{aligned}
 B_{11} &= (1/r)\sin\beta, & B_{12} &= (s/r)\sin\beta, & B_{13} &= in/r, & B_{14} &= ins/r, \\
 B_{15} &= \cos\beta/r, & B_{16} &= (s/r)\cos\beta, & B_{17} &= (s^2/r)\cos\beta, & B_{18} &= (s^3/r)\cos\beta, \\
 B_{22} &= 1, & B_{31} &= in/r, & B_{32} &= ins/r, & B_{33} &= -\sin\beta/r, & B_{34} &= 1 - (s/r)\sin\beta, \\
 B_{43} &= (in/r^2)\cos\beta, & B_{44} &= (ins/r^2)\cos\beta, & B_{45} &= n^2/r^2, \\
 B_{46} &= (n^2s/r^2) - \sin\beta/r, & B_{47} &= (n^2s^2/r^2) - (2s)\sin\beta/r, & & & & & (B.2.5) \\
 B_{48} &= (n^2s^3/r^2) - 3s^2\sin\beta/r, & B_{57} &= -2 & B_{58} &= -6s, \\
 B_{63} &= -(2/r^2)\sin\beta\cos\beta, & B_{64} &= (2/r)\cos\beta - (2s/r^2)\sin\beta\cos\beta, \\
 B_{65} &= 2insin\beta/r^2, & B_{66} &= -(2in/r) + (2ins/r^2)\sin\beta, \\
 B_{67} &= -(4ins/r) + (2ins^2/r^2)\sin\beta, & B_{68} &= -(6ins^2/r) + (2ins^3/r^2)\sin\beta,
 \end{aligned}$$

and the non-zero elements of the 8×8 matrix A_e are

$$\begin{aligned}
 A_{11} &= \cos\beta, & A_{15} &= -\sin\beta, & A_{23} &= 1, & A_{31} &= \sin\beta, & A_{35} &= \cos\beta, \\
 A_{46} &= 1, & A_{51} &= \cos\beta, & A_{52} &= L\cos\beta, & A_{53} &= -\sin\beta, & A_{54} &= -L\sin\beta, & & & (B.2.6) \\
 A_{57} &= -L^2\sin\beta, & A_{58} &= -L^3\sin\beta, & A_{63} &= 1, & A_{64} &= L, & A_{71} &= \sin\beta,
 \end{aligned}$$

$$A_{72} = L \sin \beta, \quad A_{75} = \cos \beta, \quad A_{76} = L \cos \beta, \quad A_{77} = L^2 \cos \beta, \quad A_{78} = L^3 \cos \beta,$$

$$A_{86} = 1, \quad A_{87} = 2L, \quad A_{88} = 3L^3,$$

while the non-zero elements of the 8 x 8 matrix V_r , rotary inertia being ignored, are

$$V_{11} = 1, \quad V_{12} = s, \quad V_{21} = s, \quad V_{22} = s^2, \quad V_{33} = 1, \quad V_{34} = s,$$

$$V_{43} = s, \quad V_{44} = s^2, \quad V_{55} = 1, \quad V_{56} = s, \quad V_{57} = s^2, \quad V_{58} = s^3,$$

(B.2.7)

$$V_{65} = s, \quad V_{66} = s^2, \quad V_{67} = s^3, \quad V_{68} = s^4, \quad V_{75} = s^2, \quad V_{76} = s^3,$$

$$V_{77} = s^4, \quad V_{78} = s^5, \quad V_{85} = s^3, \quad V_{86} = s^4, \quad V_{87} = s^5, \quad V_{88} = s^6.$$

B3. Dynamic Stiffness of Rib

Assembly of a number of conical shell elements to form a rib, as shown in Figure 3, for example, is a straightforward finite element computational procedure which reflects continuity of displacement and equilibrium of stresses at the nodes. When the rib has N finite element nodes the assembly results in the system matrix equation

$$Z_r(n)U_r(n) = E_r(n), \quad (B.3.1)$$

where $Z_r(n)$ is a $4N \times 4N$ system dynamic stiffness matrix, $U_r(n)$ is a $4N \times 1$ column containing the displacements of all nodes and $E_r(n)$ is a $4N \times 1$ column vector containing the nodal excitations. The subscript r refers to a complete rib. Take the inverse of equation (B.3.1) to give the system dynamic receptance matrix $Z_r(n)^{-1}$ whose ij th element is interpreted as the response at degree of freedom i due to unit excitation at degree of freedom j . The inverse can usually be computed rapidly if the elements of $Z_r(n)$ are stored in a format suitable for a band solver.

If a rib is attached to the shell at node p (usually 1) and external excitation forces are to be applied at node q , then delete all rows and columns of $Z_r(n)^{-1}$ not associated with the eight degrees of freedom at nodes p and q . The following partitioned receptance matrix results

$$\begin{bmatrix} u_p(n) \\ u_q(n) \end{bmatrix} = \begin{bmatrix} R_{pp}(n) & R_{pq}(n) \\ R_{qp}(n) & R_{qq}(n) \end{bmatrix} \begin{bmatrix} E_p(n) \\ E_q(n) \end{bmatrix} \quad (B.3.2)$$

where $u_p(n)$ and $u_q(n)$ are 4×1 column vectors of displacements at nodes p and q , respectively; $E_p(n)$ and $E_q(n)$ are column vectors of internal reaction forces and external excitations; $R_{pp}(n)$ is a 4×4 receptance matrix, whose columns are the 4×1 response vector at p due to unit excitation in turn at each of the four degrees of freedom at q .

Equation (B.3.2) can be written as the two matrix relations

$$\begin{aligned} u_p(n) &= R_{pp}(n)E_p(n) + R_{pq}(n)E_q(n), \\ u_q(n) &= R_{qp}(n)E_p(n) + R_{qq}(n)E_q(n) \end{aligned} \quad (\text{B.3.3})$$

The first of these equations is re-arranged as

$$F_p(n) = (1/2\pi r_p)R_{pp}(n)^{-1}u_p(n) - (2\pi r_p/2\pi r_p)R_{pp}(n)^{-1}R_{pq}(n)F_q(n), \quad (\text{B.3.4})$$

for line force excitations $F_p(\phi)$ and $F_q(\phi)$ at nodes p and q , respectively, $F_p(n)$ and $F_q(n)$ being the Fourier series transforms according to equation (B.2.1).

In the absence of external excitation on a rib, $F_q(n)=0$, the dynamic stiffness matrix of the rib has been defined in [3] as $F_p(n)=B(n)u_p(n)$. Noting that the rib attachment point is $r_p=a$, this gives $B(n)=(1/2\pi a)R_{pp}(n)^{-1}$, which matrix is required in the shell's spectral response of equations (2.1.1).

The second term in (B.3.4) is that part of the reaction force at point p which is due to line force excitation $F_p(n)$ on the same rib. The equivalent excitation on the shell's surface must be equal but of opposite sign. Thus

$$E(n,z) = (2\pi r_p/2\pi a)R_{pp}(n)^{-1}R_{pq}(n)F_q(n)\delta(z-z_0), \quad (\text{B.3.5})$$

where the rib attachment point is at $r=a$, $z=z_0$. The delta function has dimension m^{-1} in order to convert forces per unit length in the circumferential direction on the rib into the required forces per unit area on the shell. Take the Fourier integral transform of (B.3.5) and let the excitation be the point force vector $F_q(\phi)=F\delta(\phi-\phi_0)/r_q$ whose Fourier series transform is $F_q(n)=F\exp(-in\phi_0)/2\pi r_q$, to give

$$E(n,\alpha) = R_{pp}(n)^{-1}R_{pq}(n)F\exp(-in\phi_0 - i\alpha z_0)/2\pi a, \quad (\text{B.3.6})$$

which is the equivalent shell excitation required in Section 2.5.

The second of equations (B.3.3) can be used to calculate the displacement $u_q(n)$ at the excitation point on a rib, but this is a formidable problem as it requires the displacement of the shell $u_p(n,z=z_0)$ at the rib attachment point, which can only be obtained by evaluating a Fourier integral numerically.

Overall security classification of sheet

(As far as possible this sheet should contain only unclassified information. If it is necessary to enter classified information, the field concerned must be marked to indicate the classification, eg (R), (C) or (S))

Originator's Reference/Report No DRA TM(USGR)92326		Month October	Year 1992
Originator's Name and Location DEFENCE RESEARCH AGENCY HASLAR GOSPORT HANTS PO12 2AG			
Monitoring Agency Name and Location			
Title SOUND RADIATION FROM INFINITE LAMINATED COMPOSITE SHELL WITH PERIODIC RIB STIFFENING			
Report Security Classification UK UNCLASSIFIED		Title Classification (U,R,C or S)	
Foreign Language Title (In the case of translations)			
Conference Details			
Agency Reference		Contract Number and Period	
Project Number AS02EH14		Other References	
Authors J H JAMES			Pagination and Ref
Abstract <p>A theory of sound radiation from an infinite cylindrical shell which is stiffened periodically by ribs is given. Both shell and ribs are laminated composites. The shell is modelled by the differential equations of a thin shell theory. The flexible ribs, which exert both forces and moments on the shell's surface, are modelled by thin conical shell finite elements; degrees of freedom other than those at the shell's surface are removed by receptance methods. Excitations are time-harmonic mechanical forces at arbitrary points on the shell's surface and ribs, and acoustic monopoles in the exterior and interior fluids.</p>			
			Abstract Classification (U,, R, C or S)
Descriptors SOUND RADIATION, COMPOSITE SHELL, FIBRE REFINORCED MATERIAL, RIB STIFFENING, THEORETICAL MODEL			
Distribution Statement (Enter any limitations on the distribution of the document) UNLIMITED			

DISTRIBUTION

Copy No

Internal

USG	1
USGR	2
USGR4 (Mr James)	3
USGA	4
AWMM	5
AWMS	6
M/SR&C	7
Library, DRA Portland	8-9
Library, DRA Haslar	10-16

External

ADR(S)	17-18
CS(R)2E Navy	19
DRIC	20-49
DFP(N) Abstract Only	
DSc(Sea) Abstract Only	
DNA(SM) ADNA/SR Abstract Only	

END

FILMED

DATE:

4-93

DTIC